

Chiral and deconfinement transitions in lattice QCD with improved staggered action

A. Bazavov and P. Petreczky for HotQCD Collaboration
 Physics Department, Brookhaven National Laboratory, NY 11973 USA

We discuss chiral and deconfinement aspects of the finite temperature transition in QCD using improved staggered actions. We study different quantities related to chiral and deconfinement transition and discuss their cutoff dependence. Contrary to some earlier lattice results we find that the chiral and deconfinement transition are not closely interconnected.

1. Introduction

QCD is expected to undergo a transition to a deconfined state, where thermodynamics can no longer be described by hadronic degrees of freedom but should be described in terms of elementary quark and gluon degrees of freedom. In addition, the chiral symmetry which is broken in QCD vacuum is expected to be restored above some temperature. In the limit of zero quark masses the restoration of the chiral symmetry is expected to be a true phase transition. However, for the quark masses realized in nature this transition turns out to be an analytic crossover [1–3]. A question naturally arises whether the deconfinement and the chiral transitions are closely related. Early lattice calculations with large quark masses and/or coarse lattices suggested that deconfinement and chiral transition happen at the same temperature [4]. However, more recent investigations that use so-called stout staggered quark action and finer lattices found that these two transitions are no longer interconnected [5–7]. In this paper we are going to discuss the deconfinement and chiral transition in QCD at non-zero temperature using highly improved staggered quark (HISQ) action and tree-level improved gauge action. We refer to this combination of quark and gauge actions as HISQ/tree action. To control discretization effects calculations have been performed at three values of the lattice spacing corresponding to temporal extent $N_\tau = 6, 8$ and 12 . To fix the lattice spacing we used the r_1 scale of the static quark potential [8] and the kaon decay constant f_K . Additional calculations using the asqtad action with $N_\tau = 8$ and 12 have been performed to demonstrate the consistency of the results obtained with different actions, since the asqtad action was extensively used in the past to study QCD at non-zero temperature [1, 9, 10].

2. Chiral transition

The breaking of the chiral symmetry in QCD vacuum is signaled by non-zero expectation value of quark condensate $\langle \bar{\psi}\psi \rangle$. At non-zero temperature the quark condensate is expected to decrease, signaling the restoration of the chiral symmetry. However, the quark condensate needs a multiplicative, and for non-zero quark mass, also an additive renormalization. Therefore following Ref. [11] we consider the following quantity, which we will call the renormalized chiral condensate

$$\Delta_{l,s}(T) = \frac{\langle \bar{\psi}\psi \rangle_{l,\tau} - \frac{m_l}{m_s} \langle \bar{\psi}\psi \rangle_{s,\tau}}{\langle \bar{\psi}\psi \rangle_{l,0} - \frac{m_l}{m_s} \langle \bar{\psi}\psi \rangle_{s,0}}. \quad (1)$$

Here $\langle \bar{\psi}\psi \rangle_{l,0}$ and $\langle \bar{\psi}\psi \rangle_{l,\tau}$ refer to quark condensate at zero and non-zero temperatures, $q = l$ and s for light and strange quarks, respectively. The numerical results are shown in Fig. 1 using the lattice spacing determined by r_1 parameter and f_K . We also show the continuum estimate for $\Delta_{l,s}$ obtained with the stout action in Fig. 1. We use the value $r_1 = 0.3106\text{fm}$ [12] and $f_K = 156.1\text{MeV}$ [?] when setting the scale in MeV. When r_1 is used to set the scale we see large deviations for asqtad action, while for HISQ/tree action these deviations are largely reduced. Interestingly enough, when f_K is used to set the scale almost no cutoff effect is seen in $\Delta_{l,s}$ both for HISQ/tree and asqtad action. This feature was first noticed for stout action [6]. The difference in the stout action and our result is due to the small difference in the light quark mass m_l . In our calculation $m_l = m_s/20$, while the stout calculations correspond to $m_l = 0.037m_s$. Here m_s is the physical strange quark mass. If we perform interpolation in the quark mass using $O(N)$ scaling, which can describe the quark mass dependence of the chiral observables obtained with p4 action very well [14, 15], to the value $m_l = 0.037m_s$ we get a very good agreement with the stout results.

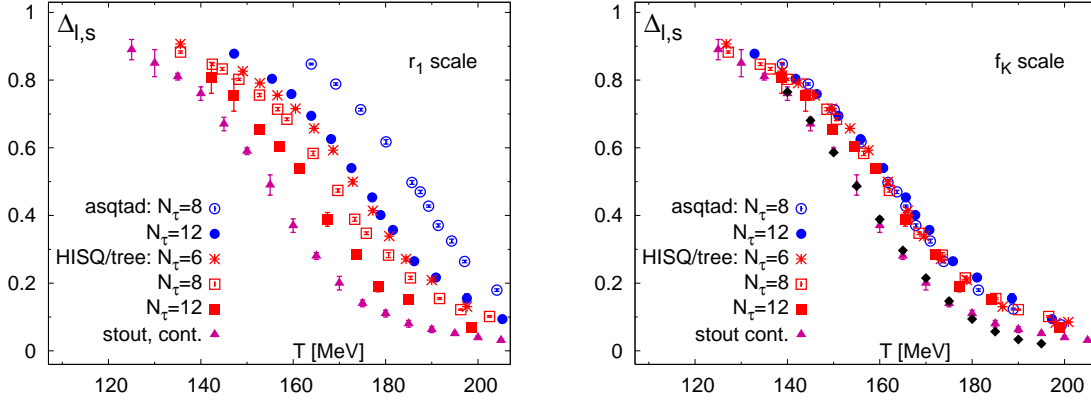


Figure 1: The subtracted chiral condensate for the asqtad and HISQ/tree actions for $m_l = m_s/20$ is compared with the continuum extrapolated data obtained with the stout action [7] (left panel). The temperature T is converted into physical units using r_1 in the left panel. In the right panel we show the temperature dependence of the same subtracted chiral condensate for the HISQ/tree and asqtad actions using f_K to set the scale. The black diamonds show HISQ/tree results for $N_\tau = 8$ after interpolation to the physical quark mass $m_l = 0.037m_s$.

3. Deconfinement transition

Quark number susceptibilities, i.e. fluctuations of the quark numbers are sensitive probe of deconfinement. These can be defined as second derivatives with respect to quark chemical potential evaluated at zero chemical potentials

$$\chi_q = \frac{T}{V} \frac{\partial^2 \ln Z}{\partial \mu_q^2} \Big|_{\mu_q=0}, \quad q = l, s. \quad (2)$$

At low temperatures quark number fluctuations are determined by massive hadrons and therefore are quite small, while at high temperatures they are determined by light quark degrees of freedom and thus proportional to T^2 . The deconfinement transition can be seen as a rapid change between these two limiting behaviors and thus the quark number susceptibilities are expected to show a rapid increase. In Fig. 2 we show the light and strange quark number susceptibilities and we clearly see the expected rapid rise in these quantities. As before the lattice spacing was fixed using r_1 and f_K . If f_K is used to fix the scale cutoff effects turn out to be very small. The rapid rise in the light quark number susceptibilities happens at temperatures, where $\Delta_{l,s}$ sharply decreases. The strange quark susceptibility shows a rapid rise at somewhat higher temperatures. Note, however, that this behavior of quark number susceptibilities is not related to different transition temperatures. The inflection points of quark number susceptibilities are dominated by the regular part of the free energy density, and the difference in the inflection points is simply due to the difference in the quark mass.

The Polyakov loop is an order parameter for the deconfinement transition in pure gauge theory, which is governed by $Z(N)$ symmetry. For QCD this symmetry is explicitly broken by dynamical quarks. There is no obvious reason for the Polyakov loop to be sensitive to the singular behavior close to the chiral limit although speculations along these lines have been made [16]. The Polyakov loop is related to the screening properties of the medium and thus to deconfinement. After proper renormalization, the square of the Polyakov loop characterizes the long distance behavior of the static quark anti-quark free energy; it gives the excess in free energy needed to screen two well-separated color charges. The renormalized Polyakov loop has been studied in the past in pure gauge theory [17, 18] as well as in QCD with two [19], three [20] and two plus one flavors [10, 11]. The renormalized Polyakov loop, calculated on lattices with temporal extent N_τ , is obtained from the bare Polyakov loop

$$L_{ren}(T) = z(\beta)^{N_\tau} L_{bare}(\beta) = z(\beta)^{N_\tau} \left\langle \frac{1}{3} \text{Tr} \prod_{x_0=0}^{N_\tau-1} U_0(x_0, \vec{x}) \right\rangle, \quad (3)$$

where $z(\beta) = \exp(-c(\beta)/2)$ and $c(\beta)$ is the additive normalization of the static potential chosen such that it coincides with the string potential at distance $r = 1.5r_0$ with r_0 being the Sommer scale. The numerical results

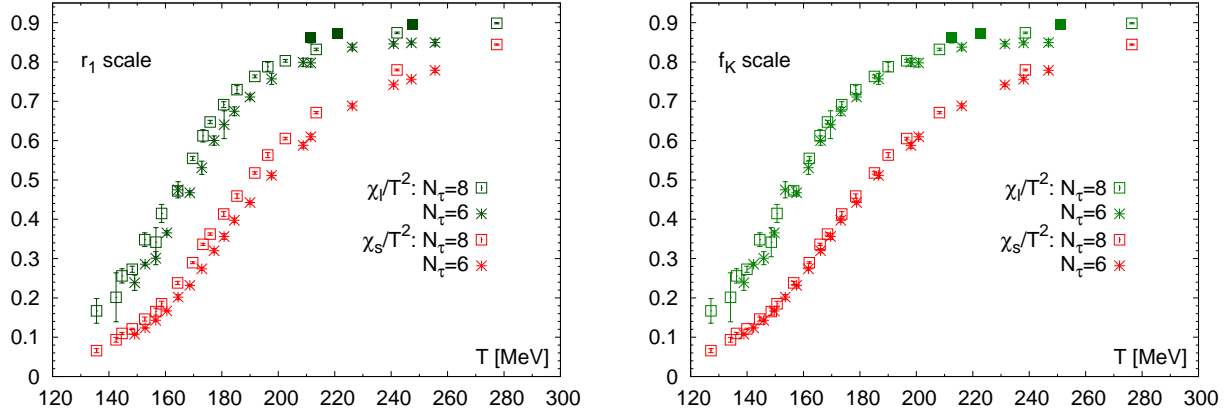


Figure 2: Light quark number susceptibilities calculated for the asqtad and HISQ/tree actions and compared with the strange quark number susceptibility. In the left panel r_1 is used to set the lattice scale, while in the right panel we use f_K . The filled squares correspond to $N_\tau = 12$.

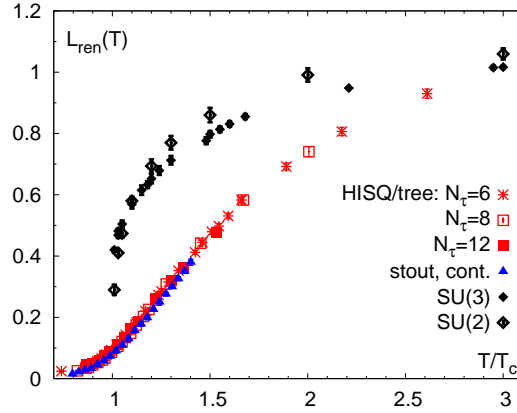


Figure 3: The renormalized Polyakov loop as function of T/T_c (right). For the HISQ/tree data we used the values of T_c discussed in [21], while for stout data we used the value of $T_c = 157$ MeV from the inflection point of renormalized chiral condensate [7].

for the renormalized Polyakov loop for the HISQ/tree action are shown in the right panel of Fig. 3 as function of T/T_c , with T_c being the transition temperature. As one can see from the figure the cutoff (N_τ) dependence of the renormalized Polyakov loop is small. We also compare our results with the continuum extrapolated stout results [7] and the corresponding results in pure gauge theory [17, 18]. We find good agreement between our results and the stout results. We also see that in the vicinity of the transition temperature the behavior of the renormalized Polyakov loop in QCD and in the pure gauge theory is quite different.

4. Conclusion

In this contribution we discussed different quantities, which characterize the deconfinement and chiral transition in QCD at non-zero temperature and studied their cutoff dependence. We showed that when the kaon decay constant f_K is used to set the scale (lattice spacing) the cutoff effects in different quantities are quite small and calculations performed with the asqtad and HISQ/tree actions are in good agreement with calculations performed with the stout action. We pointed out that it is difficult to define the deconfinement temperature. Different observables that are used to characterize the deconfinement transition show rapid rise at different temperatures, which in turn, could be different from the chiral transition temperature. This is due to the fact that the observables used to study the deconfinement transition are not sensitive to the singular part of the free

energy density or have limited sensitivity to it.

Acknowledgments

This work has been supported in part by contracts DE-AC02-98CH10886 and DE-FC02-06ER-41439 with the U.S. Department of Energy and contract 0555397 with the National Science Foundation. The numerical calculations have been performed using the USQCD resources at Fermilab as well as the BlueGene/L at the New York Center for Computational Sciences (NYCCS).

References

- 1 C. Bernard *et al.* [MILC Collaboration], Phys. Rev. D **71**, 034504 (2005)
- 2 Y. Aoki, *et al.*, Nature **443**, 675 (2006). [hep-lat/0611014].
- 3 M. Cheng *et al.*, Phys. Rev. D **74**, 054507 (2006)
- 4 P. Petreczky, Nucl. Phys. Proc. Suppl. **140**, 78-91 (2005).
- 5 Y. Aoki *et al.*, Phys. Lett. B **643**, 46 (2006)
- 6 Y. Aoki *et al.*, JHEP **0906**, 088 (2009)
- 7 S. Borsanyi *et al.* [Wuppertal-Budapest Collaboration], JHEP 1009, 073 (2010)
- 8 C. Aubin *et al.*, Phys. Rev. D **70**, 094505 (2004).
- 9 C. Bernard *et al.*, Phys. Rev. D **75**, 094505 (2007)
- 10 A. Bazavov *et al.* (HotQCD Collaboration), Phys. Rev. D **80**, 014504 (2009)
- 11 M. Cheng *et al.*, Phys. Rev. D **77**, 014511 (2008)
- 12 A. Bazavov *et al.*, PoS LATTICE2010, 074 (2010)
- 13 J. Rosner, in K. Nakamura *et al.*, (Particle Data Group), J. Phys. G 37, 075021 (2010)
- 14 S. Ejiri *et al.*, Phys. Rev. D **80**, 094505 (2009)
- 15 O. Kaczmarek *et al.*, Phys. Rev. **D83**, 014504 (2011). [arXiv:1011.3130 [hep-lat]].
- 16 see e.g. Y. Hatta and K. Fukushima, arXiv:hep-ph/0311267, and references therein.
- 17 O. Kaczmarek *et al.*, Phys. Lett. **B543**, 41-47 (2002).
- 18 S. Digal, S. Fortunato, P. Petreczky, Phys. Rev. **D68**, 034008 (2003).
- 19 O. Kaczmarek, F. Zantow, Phys. Rev. **D71**, 114510 (2005).
- 20 P. Petreczky, K. Petrov, Phys. Rev. **D70**, 054503 (2004).
- 21 A. Bazavov and P. Petreczky, [arXiv:1107.5027 [hep-lat]].